Research on Biomedical Engineering
rbejournal.org
Volume 31, Number 4, p. 313-318, 2015

Original Article
DOI: http://dx.doi.org/10.1590/2446-4740.0630

Investigation of the influence of design details on short implant biomechanics using colorimetric photoelastic analysis: a pilot study

João César Zielak*, Felipe Belmonte Archetti, Ricardo Scotton, Marcelo Filietaz, Carmen Lucia Mueller Storrer, Allan Fernando Giovanini, Tatiana Miranda Deliberador

Abstract **Introduction**: The clinical survival of a dental implant is directly related to its biomechanical behavior. Since short implants present lower bone/implant contact area, their design may be more critical to stress distribution to surrounding tissues. Photoelastic analysis is a biomechanical method that uses either simple qualitative results or complex calculations for the acquisition of quantitative data. In order to simplify data acquisition, we performed a pilot study to demonstrate the investigation of biomechanics via correlation of the findings of colorimetric photoelastic analysis (stress transition areas; STAs) of design details between two types of short dental implants under axial loads. **Methods**: Implants were embedded in a soft photoelastic resin and axially loaded with 10 and 20 N of force. Implant design features were correlated with the STAs (mm^2) of the colored fringes of colorimetric photoelastic analysis. **Results**: Under a 10 N load, the surface area of the implants was directly related to STA, whereas under a 20 N load, the surface area and thread height were inversely related to STA. **Conclusion**: A smaller external thread height seemed to improve the biomechanical performance of the short implants investigated.

Keywords: Biomechanics, Dental implants, Dental stress analysis, Short implants.

Introduction

Stress distribution around implants is completely different than that around natural teeth. The existence of the periodontal ligament, for example, exerts a great influence on the biomechanical behavior of teeth. Moreover, although there is a physiological limit of tolerance for the stress linked to bone resorption, marginal chronic bone loss around implants may happen over time (Chun et al., 2002; Goodacre et al., 2003; Haruta et al., 2011; Khayat et al., 2013; Romanos et al., 2014; Tada et al., 2003). This loss can be attributed to surgical trauma, inflammation, excessive micromovements, and loading conditions. Of these, loading conditions are considered one of the most critical factors influencing bone loss (Sakka and Coulthard, 2011; Ueda et al., 2004).

Several reports state that marginal bone loss can be avoided by the use of certain design concepts such as platform switching. According to this concept, abutments should have a narrower diameter than the implant platform itself (Bilhan et al., 2010; Dursun et al., 2014; Sakka and Coulthard, 2011; Vandeweghe and De Bruyn, 2012). In addition, there are other implant features that have proven to be effective for bone maintenance. A short implant length (e.g., < 10 mm) (Monje et al., 2013) can be used to reduce surgical risks related to undesirable positions or inclinations (Assenza et al., 2003; Stellingsma et al., 2004) as well as to avoid advanced bone graft procedures (Chang et al., 2012). A systematic review has shown that there can be more complications in patients with severe bone loss treated with vertical bone augmentation than in those treated with short dental implants (Esposito et al., 2009). Since most manufacturers worldwide produce short implants, it is important that clinicians understand their biomechanical behavior, which may influence clinical outcomes.

The literature describes photoelastic biomechanical analysis as a method often employed to assess the stress distribution around implants (Lopes et al., 2011; Silva et al., 2010; Ueda et al., 2004). However, although photoelastic analysis provides good qualitative evaluation of tension distribution (e.g., critical stress points), it may not be a practical test for quantitative assessment, especially because of the complex mathematic calculations that are necessary (Assunção et al., 2009). Photoelastic analysis is based on the property of transparent materials that allows them to produce images with colored fringes when subjected to load and visualized under polarized light (Lopes et al., 2011). In this analysis, the color magenta (red to blue) represents the color of fringe transition in first fringes (Ueda et al., 2004). Therefore,

*e-mail: jzielak2@gmail.com
Received: 10 October 2014 / Accepted: 08 October 2015

if stress concentration is related to the proximity of the fringes, the hypothesis of the present study is that the area occupied by this transition color is directly related to stress distribution. In turn, this can be used as quantitative data that is easily obtained from photoelastic testing. A smaller area of magenta is related to a higher concentration of stress, and a larger area is related to a lower concentration of stress. Thus, the aim of the current pilot study was to analyze the biomechanics of short implants by correlating the findings of colorimetric photoelastic analysis (stress transition areas; STAs) with design details in two different types of short dental implants under axial loads.

Methods

Two samples from two different manufacturers of short implants were connected to their abutments (Table 1) and embedded in soft photoelastic resin (40 × 50 mm Flexivel GIII; Polipox, Sao Paulo, SP, Brazil). All implants were subjected to axial loads of 10 and 20 N for approximately 3 seconds in a universal testing machine (EMIC, Sao Jose dos Pinhais, Paraná, Brazil) coupled to a polariscope (Optovac, Osasco, SP, Brazil). The tension fringes produced were photographed with a digital camera (Canon 3Ti; Canon, Melville, NY, USA) and a 105 mm macro lens (Sigma, Ronkonkoma, NY, USA). Only half of the total image field was used for analysis (14 × 5 mm, 300 dpi). From these images, several parameters were obtained and measured using image analysis software (Image Tool 3.0; UTCH, Houston, Texas, United States). Surface area (SA) was calculated using Equation 1.

$$SA = \frac{2r \cdot \pi \cdot h}{2} \quad (1)$$

Where: $2r$ = implant diameter and h = implant length.

The mean thread height (MTH = sum of heights of all threads divided by the number of threads) (Figure 1), mean thread distance (MTD = sum of all distances between the threads of all implants divided by the number of distances measured) (Figure 1), STA (= area of magenta color [red to blue] selected from the images by Adobe Photoshop 7.0 image analysis software; Adobe, San Jose, California, USA) (Figures 2a and 3a), maximum distance from the surface of the implant to the STA (MDS) both laterally and apically (Figures 2b and 3b), and number of software-detected STAs (NTA) of each implant design were also measured. The measuring error of the technique was 3-5% due to dimensional changes of the resin. All photographs were taken by the same operator, using the same camera, and with the same resolution. Selection of the magenta color was carried out by the same software installed on a single personal computer. Even though the borders of the selected color did not present straight lines (Figures 1a and 2a), a feature of the software guaranteed a measurement pattern and no error deviation was detected.

In this single sample analysis, all data (SA, MTH, MTD, STA, and MDS) were subjected to regression analysis in order to evaluate possible correlations using SigmaPlot 12 software (Systat, San Jose, California, USA).

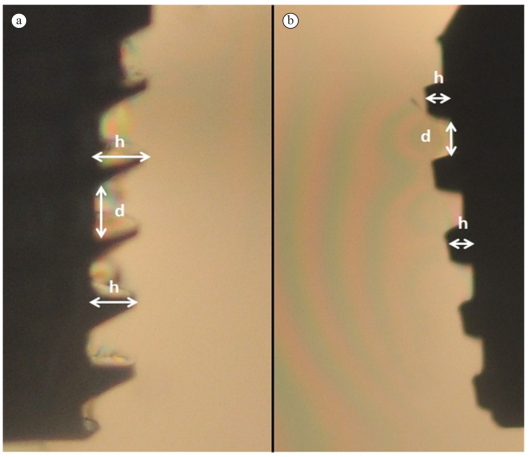

Figure 1. Image parameters for measurement of thread height and thread distance. (a) External hexagon implant (3.8 × 6.0 mm); (b) Frictional-abutment implant (3.75 × 6.0 mm). H = height, d = distance between threads.

Table 1. Features of the short dental implants used in the current study.

Manufacturer	n	Implant features		Platform features		Abutment features
		Diameter (mm)	Length (mm)	CT	Dimensions (mm)	Dimensions (mm)
A	1	3.8	6	EH	4.1	4.1 × 11
	1	5.0		EH/PS		
B	1	3.75		F/PS	2.9	2-4.5 × 13*
	1	5.0			4.4	3-4.5 × 13*

A = DSP™: Dental Special Products, Campo Largo, PR, Brazil. B = Kopp™: Sistema de Implantes, Curitiba, PR, Brazil. CT = Connection type with abutment. EH = External hexagon. PS = Platform switching. F = Frictional. *At the platform level, both abutments started from the lower diameter to an emergence profile of 4.5 mm.

Results

In this study, as the load increased, fringes were observed farther from the implant surface and were apically directed. All measurements are reported in Table 2. Correlations were observed only between SA and STA and between MTH and STA. SA and STA showed a direct correlation when a load of 10 N was applied (r = 0.959) (Figure 4), but no correlation was observed when a load of 20 N was applied (r = 0.176).

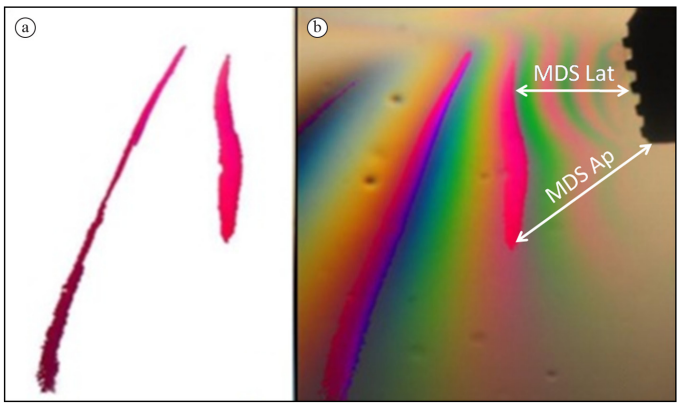

Figure 2. Images of frictional-abutment implant (3.75 × 6 mm) loaded with 10 N. (a) Software-selected stress transition areas; (b) Polarized image of implant with software-selected stress transition areas (magenta). MDS Lat = Maximum distance from the lateral implant surface to the stress transition area (magenta). MDS Ap = Maximum distance from the apical implant surface to the stress transition area (magenta).

Table 2. Implant features and post-loading characteristics.

Implant features					Load	Post-loading data			
CT	ID (mm)	SA (mm^2)	MTH (mm)	MTD (mm)	L (N)	STA (mm^2)	MDS (mm)		NTA
							Lat	Ap	
F	3.75 × 6	68.67	0.28	0.46	10	5.84	8.85	17.52	2
EH	3.8 × 6	72.99	1.78	1.68		6.00	21.54	59.17	2
EH	5 × 6	111.18	1.65	1.84		6.13	28.25	55.11	2
F	5 × 6	135.61	1.21	2.51		6.36	7.52	15.40	2
F	3.75 × 6	68.67	0.28	0.46	20	7.80	49.79	89.22	2
F	5 × 6	135.61	1.21	2.51		5.47	41.54	72.78	2
EH	5 × 6	111.18	1.65	1.84		5.05	43.08	80.88	2
EH	3.8 × 6	72.99	1.78	1.68		3.68	33.72	74.80	2

CT = Connection type with abutment. F = Frictional. EH = External hexagon. ID = Implant dimensions. SA = Surface area. MTH = Mean thread height. MTD = Mean thread distance. L = Load. STA = Stress transition area. MDS = Maximum distance from implant surface to stress transition area. Lat = Laterally. Ap = Apically. NTA = Total number of (software-detected) stress transition areas.

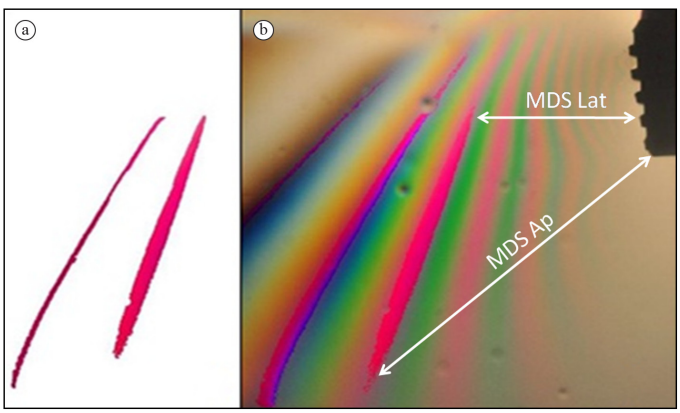

Figure 3. Photoelastic images of frictional-abutment implant (3.75 × 6 mm) loaded with 20 N. (a) Software-selected stress transition areas; (b) Polarized image of implant with software-selected stress transition areas (magenta). MDS Lat = Maximum distance from the lateral implant surface to the stress transition area (magenta). MDS Ap = Maximum distance from the apical implant surface to the stress transition area (magenta).

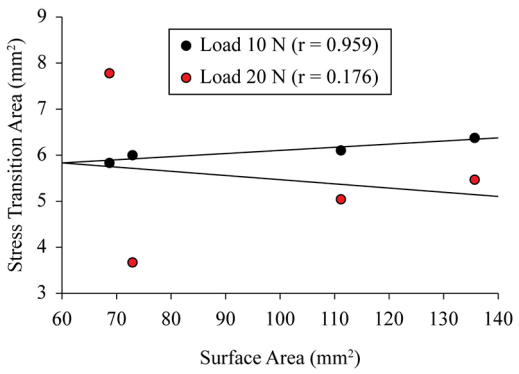

Figure 4. Correlation between stress transition area and surface area in loading situations of 10 and 20 N. At 10 N only, an increase in surface area led to an increase in stress transition area. The largest surface area produced the lowest stress concentration.

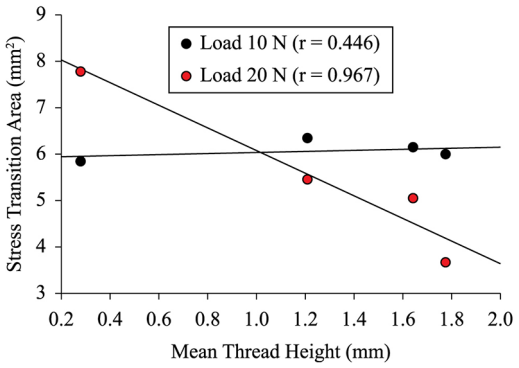

Figure 5. Correlation between stress transition area and mean thread height in loading situations of 10 and 20 N. At 20 N only, the largest mean thread height led to a decrease of total transition area, indicating a concentration of stress in this situation.

When the relationship between MTH and STA was analyzed (Figure 5), a weak correlation was found when a load of 10 N was applied (r = 0.446), whereas a strong negative correlation was observed when a 20 N load was applied (r = –0.967).

Discussion

Although photoelastic resins are much more resilient than human bone, the physical characteristics of the photoelastic resin used in the current study meant that high stress loads (10 and 20 N) could be applied to allow the study of the biomechanical properties of dental implants under these conditions. The present pilot study represents the development of a simpler methodology for photoelastic analysis; the next step will be the demonstration of the same methodology applied to larger numbers of specimens, which will allow statistical analysis of the results.

In this study, the transition areas of the first fringes (magenta color) were selected easily from the images by the software used, which made this measurement a possible marker for the quantitative representation of the distribution of stress. Since the STA represents a stress relief region between two fringes (Ueda et al., 2004), it could be assumed that a higher STA value indicates higher stress dissipation, which is equivalent to lower stress concentration.

As shown in Figures 1 and 2 and Table 2 (MDS values), an increase in load increased the extent or distance of the biomechanical influence around the implant; this can also occur in clinical situations. Another important influence on stress distribution that should be considered is the length of time of load application (Maeda et al., 2007; Menicucci et al., 2002). The present study used only 3 seconds of load application in a homogenous material (photoelastic resin). To extrapolate the results observed to a clinical situation, it is necessary to consider that the ability of local bone to support high loads depends on bone quality. Thus, quantification of the amount of force that could cause overload in a specific clinical case becomes very difficult (Çehreli et al., 2004; Lesmes and Laster, 2011; Teixeira et al., 2010).

In the present study, when a 10 N load was applied, no correlation was observed between MTH or MTD and STA. Even though there was a strong correlation with SA, differences among the STA results were small (5.84, 6.00, 6.13, and 6.36 mm²) (Table 2, Figure 4). A previous study using the same methodology but with regular width implants and a lower load showed that although a positive correlation was observed, different surface areas were related to distinctive magenta areas (Zielak et al., 2013). Due to the similar results of all of the implants tested (Figure 4, r = 0.959), the data of the present study appear to be in agreement with those of a study in which the implant diameter, linked to the calculation of surface area, did not influence the stress distribution of vertical loads (Chang et al., 2012). On the other hand, here, the lowest implant diameter and consequently the lowest SA value (68.67 mm²) was related to the highest STA value under a load of 20 N. However, our findings need a more refined approach to be better understood. With an increase in load (20 N), the results can be clarified if other features of the implants are examined. As seen in Table 2, there was a weak correlation between MTD and STA (r = –0.365), but extreme STA values were strongly related to MTH (Figure 5) (r = 0.967). A MTH value of 1.78 mm corresponded to a STA value of 3.68 mm² and a MTH value of 0.28 mm (approximately 6.4 times lower) corresponded to a STA value of 7.80 mm², indicating more than double

the capacity for stress distribution. It is known that a small thread height, or as it is commonly called a low pitch, can help to optimize stress distribution (Baggi et al., 2013). Although this feature may not be critical for regular width implants, a trend in the correlation between MTH and magenta areas has been demonstrated previously (Zielak et al., 2013). Thus, some authors suggest that implant threads must have a square shape and a small radius in order to optimize the biomechanical behavior of implants (Chun et al., 2002; Tada et al., 2003), which in turn can influence osseointegration and bone stability (Duaibis et al., 2012; Orsini et al., 2012).

The higher stress distribution capacity observed (STA = 7.80 mm^2) can also be explained based on the fact that the implant with the lowest MTH (0.28 mm) also had the lowest MTD (0.46 mm), a feature that is regularly applied to increase bone stability around the cervical area of dental implants (Rismanchian et al., 2010). In addition, micro-threads have been studied to aid the distribution of stress around dental implants (Choi et al., 2012). These characteristics may all be related to the external surface of the implant, and thus manufacturers must carefully address these issues when preparing short implants. Considering the limitations of photoelastic analysis itself, an important feature of this methodology is represented by its quantitative results. Although photoelastic and finite element studies currently present qualitative results or descriptive statistics (Rossi et al., 2014), an increase in the number of specimens of equal dimensions applied within this methodology may demonstrate even more conclusive findings.

Under a load of up to 10 N, an increase in implant SA was directly related to an increase in stress distribution, as shown by the increase in fringe transition areas (magenta color). When the load was increased to 20 N, the lowest stress concentration value was directly related to the lowest SA associated with the lowest MTH and lowest MTD. Therefore, design details such as the height and interval of threads may play important roles in the biomechanics of short dental implants. Moreover, according to the analysis of the present study, a smaller external thread height seemed to improve the biomechanical performance of short dental implants.

References

Assenza B, Scarano A, Petrone G, Iezzi G, Thams U, San Roman F, Piattelli A. Crestal bone remodeling in loaded and unloaded implants and the microgap: a histologic study. Implant Dentistry. 2003; 12(3):235-41. http://dx.doi.org/10.1097/01.ID.0000074081.17978.7E. PMid:14560484.

Assunção WG, Barão VAR, Tabata LF, Gomes EA, Delbem JA, Santos PH. Biomechanics studies in dentistry: bioengineering applied in oral implantology. The Journal of Craniofacial Surgery. 2009; 20(4):1173-7. http://dx.doi.org/10.1097/SCS.0b013e3181acdb81. PMid:19568186.

Baggi L, Girolamo M, Vairo G, Sannino G. Comparative evaluation of osseointegrated dental implants based on platform-switching concept: influence of diameter, length, thread shape, and in-bone positioning depth on stress-based performance. Computational and Mathematical Methods in Medicine. 2013; 2013:250929. http://dx.doi.org/10.1155/2013/250929.

Bilhan H, Mumcu E, Erol S, Kutay Ö. Influence of platform-switching on marginal bone levels for implants with mandibular overdentures: a retrospective clinical study. Implant Dentistry. 2010; 19(3):250-8. http://dx.doi.org/10.1097/ID.0b013e3181dc9d1a. PMid:20523181.

Çehreli M, Sahin S, Akça K. Role of mechanical environment and implant design on bone tissue differentiation: current knowledge and future contexts. Journal of Dentistry. 2004; 32(2):123-32. http://dx.doi.org/10.1016/j.jdent.2003.09.003. PMid:14749084.

Chang SH, Lin CL, Hsue SS, Lin YS, Huang SR. Biomechanical analysis of the effects of implant diameter and bone quality in short implants placed in the atrophic posterior maxilla. Medical Engineering & Physics. 2012; 34(2):153-60. http://dx.doi.org/10.1016/j.medengphy.2011.07.005. PMid:21807548.

Choi KS, Park SH, Lee JH, Jeon YC, Yun MJ, Jeong CM. Stress distribution on scalloped implants with different microthread and connection configurations using three-dimensional finite element analysis. The International Journal of Oral & Maxillofacial Implants. 2012; 27(3):e29-38. PMid:22616069.

Chun HJ, Cheong SY, Han JH, Heo SJ, Chung JP, Rhyu IC, Choi YC, Baik HK, Ku Y, Kim MH. Evaluation of design parameters of osseointegrated dental implants using finite element analysis. Journal of Oral Rehabilitation. 2002; 29(6):565-74. http://dx.doi.org/10.1046/j.1365-2842.2002.00891.x. PMid:12071926.

Duaibis R, Kusnoto B, Natarajan R, Zhao L, Evans C. Factors affecting stresses in cortical bone around miniscrew implants: a three-dimensional finite element study. The Angle Orthodontist. 2012; 82(5):875-80. http://dx.doi.org/10.2319/111011-696.1. PMid:22390634.

Dursun E, Tulunoglu I, Ozbek SM, Uysal S, Akalın FA, Kilinc K, Karabulut E, Tözüm TF. The influence of platform switching on clinical, laboratory, and image-based measures: a prospective clinical study. Clinical Implant Dentistry and Related Research. 2014; 16(6):936-46. http://dx.doi.org/10.1111/cid.12054. PMid:23490454.

Esposito M, Grusovin MG, Felice P, Karatzopoulos G, Worthington HV, Coulthard P. Interventions for replacing missing teeth: horizontal and vertical bone augmentation techniques for dental implant treatment. Cochrane Database of Systematic Reviews. 2009; 7(4):CD003607. http://dx.doi.org/10.1002/14651858. PMid:19821311.

Goodacre CJ, Bernal GB, Rungcharassaeng K, Kan JY. Clinical complications with implants and implant prostheses. The Journal of Prosthetic Dentistry. 2003; 90(2):121-32. http://dx.doi.org/10.1016/S0022-3913(03)00212-9. PMid:12886205.

Haruta A, Matsushita Y, Tsukiyama Y, Sawae Y, Sakai N, Koyano K. Effects of mucosal thickness on the stress distribution and denture stability of mandibular implant-supported overdentures with unsplinted attachments in vitro. Journal of Dental Biomechanics. 2011; 2011:894395. http://dx.doi.org/10.4061/2011/894395.

Khayat PG, Arnal HM, Tourbah BI, Sennerby L. Clinical outcome of dental implants placed with high insertion torques (up to 176 Ncm). Clinical Implant Dentistry and Related Research. 2013; 15(2):227-33. http://dx.doi.org/10.1111/j.1708-8208.2011.00351.x. PMid:21599832.

Lesmes D, Laster Z. Innovations in dental implant design for current therapy. Oral and Maxillofacial Surgery Clinics of North America. 2011; 23(2):193-200 http://dx.doi.org/10.1016/j.coms.2011.02.001. PMid:21492795.

Lopes MB, Valarini N, Moura SK, Guiraldo RD, Gonini A Jr. Photoelastic analysis of stress generated by a silorane-based restoration system. Brazilian Oral Research. 2011; 25(4):302-6. http://dx.doi.org/10.1590/S1806-83242011000400004. PMid:21860916.

Maeda Y, Miura J, Taki I, Sogo M. Biomechanical analysis on platform switching: is there any biomechanical rationale? Clinical Oral Implants Research. 2007; 18(5):581-4. http://dx.doi.org/10.1111/j.1600-0501.2007.01398.x. PMid:17608737.

Menicucci G, Mossolov A, Mozzati M, Lorenzetti M, Preti G. Tooth-implant connection: some biomechanical aspects based on finite element analysis. Clinical Oral Implants Research. 2002; 13(3):334-41. http://dx.doi.org/10.1034/j.1600-0501.2002.130315.x. PMid:12010166.

Monje A, Fu JH, Chan HL, Suarez F, Galindo-Moreno P, Catena A, Wang HL. Do implant length and width matter for short dental implants (6-9 mm)? A meta-analysis of prospective studies. Journal of Periodontology. 2013; 84(12):1783-91. http://dx.doi.org/10.1902/jop.2013.120745. PMid:23451988.

Orsini E, Giavaresi G, Trire A, Ottani V, Salgarello S. Dental implant thread pitch and its influence on the osseointegration process: an in vitro comparison study. The International Journal of Oral & Maxillofacial Implants. 2012; 27(2):383-92. PMid:22442779.

Rismanchian M, Birang R, Shahmoradi M, Talebi H, Zare RJ. Developing a new dental implant design and comparing its biomechanical features with four designs. Dental Research Journal. 2010; 7(2):70-5. PMid:22013460.

Romanos GE, Malmstrom H, Feng C, Ercoli C, Caton J. Immediately loaded platform-switched implants in the anterior mandible with fixed prostheses: a randomized, split-mouth, masked prospective trial. Clinical Implant Dentistry and Related Research. 2014; 16(6):884-92. http://dx.doi.org/10.1111/cid.12065. PMid:23551623.

Rossi AC, Freire AR, Prado FB, Asprino L, Correr-Sobrinho L, Caria PHF. Photoelastic and finite element analyses of occlusal loads in mandibular body. Anatomy Research International. 2014; 2014:174028. http://dx.doi.org/10.1155/2014/17402.

Sakka S, Coulthard P. Implant failure: etiology and complications. Medicina Oral, Patologia Oral y Cirugia Bucal. 2011; 16(1):e42-4. http://dx.doi.org/10.4317/medoral.16.e42. PMid:20526267.

Silva DP, Cazal C, Almeida FC, Dias RB, Ballester RY. Photoelastic stress analysis surrounding implant-supported prosthesis and alveolar ridge on mandibular overdentures. International Journal of Dentistry. 2010; 2010:780670. http://dx.doi.org/10.1155/2010/780670.

Stellingsma C, Vissink A, Meijer HJA, Kuiper C, Raghoebar GM. Implantology and the severely resorbed edentulous mandible. Critical Reviews in Oral Biology and Medicine. 2004; 15(4):240-8. http://dx.doi.org/10.1177/154411130401500406. PMid:15284188.

Tada S, Stegaroiu R, Kitamura E, Miyakawa O, Kusakari H. Influence of implant design and bone quality on stress/strain distribution in bone around implants: a 3-dimensional finite element analysis. The International Journal of Oral & Maxillofacial Implants. 2003; 18(3):357-68. PMid:12814310.

Teixeira MF, Ramalho SA, Sartori IAM, Lehmann RB. Finite element analysis of 2 immediate loading systems in edentulous mandible: rigid and semirigid splinting of implants. Implant Dentistry. 2010; 19(1):39-49. http://dx.doi.org/10.1097/ID.0b013e3181cc7ffc. PMid:20147815.

Ueda C, Markarian RA, Sendyk CL, Laganá DC. Photoelastic analysis of stress distribution on parallel and angled implants after installation of fixed prostheses. Brazilian Oral Research. 2004; 18(1):45-52. http://dx.doi.org/10.1590/S1806-83242004000100009. PMid:15273786.

Vandeweghe S, De Bruyn H. A within-implant comparison to evaluate the concept of platform switching: a randomized controlled trial. European Journal of Oral Implantology. 2012; 5(3):253-62. PMid:23000709.

Zielak JC, Filietaz M, Archetti FB, Camati PR, Verbicaro T, Scotton R, Furuse AY, Gonzaga CC. Colorimetric photoelastic analysis of tension distribution around dental implants. Revista Sul-Brasileira de Odontologia. 2013; 10(4):318-25.

Authors

João César Zielak[1]*, Felipe Belmonte Archetti[2], Ricardo Scotton[1], Marcelo Filietaz[1], Carmen Lucia Mueller Storrer[1], Allan Fernando Giovanini[1], Tatiana Miranda Deliberador[1]

[1] Graduate Program in Dentistry, Universidade Positivo, Rua Prof. Pedro Viriato Parigot de Souza, 5300, Campo Comprido, CEP 81280-330, Curitiba, PR, Brazil.

[2] Graduate Program in Dentistry, Universidade Federal do Paraná – UFPR, Curitiba, PR, Brazil.